VOL. 11, NO. 21, NOVEMBER 2016 ISSN 1819-6608
ARPN Journal of Engineering and Applied Sciences

www.arpnjournals.com

# ELECTROCHEMICAL METHODS, SEM-EDS AND AFM STUDIES FOR ASSESSING CORROSION INHIBITION OF CARBON STEEL IN ACIDIC MEDIA

Qhatan A. Yousif and Adel A. Al-Zhara
Department of Chemistry, College of Science, University of Al-Qadisiyah, Al-Qadisiyah, Iraq
E-Mail: Qahtan.Adnan@qu.edu.iq

**ABSTRACT**

The effect of the acriflavine inhibitor and silicon dioxide nanoparticles on the corrosion of carbon steel in 0.25 M hydrochloric acid have been studied using the open circuit potential (OCP), potentiodynamic polarization (PDP), scanning electron microscopy (SEM), energy dispersive spectroscopy (EDS) and atomic force microscopy (AFM) techniques. It was observed that the corrosion inhibition effect on the steel electrode is enhanced in the presence of silica nanoparticles which form a protective layer on the electrode surface. The results showed that acriflavine inhibitor is a good inhibitor, which acts as a mixed-type inhibitor control for carbon steel, and the inhibition increases in the presence of silica nanoparticles. The images from SEM and EDS analyses indicate the formation of films on the surface electrode, while the AFM measurements confirmed that the average roughness value reduces which refers to the protection layer. The kinetic parameters for the corrosion process have been calculated and are discussed.

**Keywords:** acriflavine, silica nanoparticles, corrosion inhibition, carbon steel.

## 1. INTRODUCTION

Carbon steel is one of the main construction materials, which is used widely in the chemical industry and related industries, which deal with acidic and alkaline solutions and salt [1]. Owing to the increase in the number of industrial applications of steel in acidic solutions, the study of the phenomenon of metal corrosion in acidic solutions is thus very important [2]. The chief problem with the use of carbon steel is dissolution in acidic solutions [3] and this is a particular problem as hydrochloric acid is often used for the pickling of iron and its alloys *i.e.* for the removal of rust or any scale formed on the surface of the metal. In order to prevent or delay this, corrosion inhibitors are often used [4], which reduces acid consumption. Heterogeneous inhibitors, especially based on organic compounds are commonly used to reduce the corrosion of carbon steel in acidic media, and in particular to protect the corrosion of oil and gas pipelines[5,6]. Through the growth of nanotechnology, there are a number of reports of $ZrO_2$, $Al_2O_3$, SiC and $TiO_2$ nanoparticles that have been added to the plating bath to form nano-composite coatings [7]. Silicates have been used as corrosion inhibitors for iron and its alloys in acidic solution and act to protect the metal surface through the formation of a coating composed of gel hydrated silica and iron oxides [8] as well as the deposition of the thin layer of silicate on the surface of the carbon steel [10,11]. The insoluble $SiO_2$ nanoparticles are used as reinforcement for many industrial applications, due to their hardness[11], excellent chemical stability and high resistance to oxidation [12]. However, given the size of nanometric particles, agglomeration of the $SiO_2$ occurs very easily in the plating bath, which in turn promotes conglomeration on the deposited alloy and failure of the nanocomposite coatings. Therefore, the dispersion of the particles in the coating bath is an important parameter that is influenced both by the concentration of the nanoparticles and the stirring rate[13]. The aim of the present paper focuses on a study the effect of the silicate nanoparticles with acriflavine inhibitor on the carbon steel in 0.25 M HCl acidic solution by electrochemical methods. The thermodynamic and kinetics parameters of corrosion inhibition and the development of surface morphology are studied by SEM, EDX and AFM techniques.

## 2. METHODOLOGY DETAILS

### 2.1. preparation of working electrode and corrosion inhibition study

The working electrode which used in this study is formed from carbon steel obtained from Iraq's oil field. Table-1 shows the chemical composition of samples of carbon steel as analysed by optical emission microscopy (PIM MASTER PRO2, OXFORD Company, UK). To prepare the samples, the pipe is first cut (dimensions 1cm × 1cm with thickness 1 cm) and a braided with SiC emery papers of different sizes and covered with epoxy to expose a section area 1 $cm^2$ to the acidic solution. After polishing the samples with $Al_2O_3$ paste to obtain a mirror-like surface on the electrode surface, the electrode was cleaned using hot benzene (*N.B.* care this is a potential carcinogen), acetone and finally with distilled water and dried.

**Table-1.** Carbon steel chemical composition.

| Elements | C | Si | Mn | Cr | Mo | Ni | Cu | Fe |
|---|---|---|---|---|---|---|---|---|
| Wt.% | 2.180 | 3.100 | 1.360 | 0.102 | 0.127 | 0.213 | 0.596 | Balance |

A study was performed of the action of a variety of inhibitors towards the corrosion of carbon steel in 0.25 M HCl in the presence of $3 \times 10^{-3}$ M of acriflavine at 298.15K. The following reagents were used: acriflavine

(obtained from SIGMA-ALDRICH Company, Figure-1) and $SiO_2$ nanoparticles (0.05g) were formed in corrosion inhibition solution. The solution for all experiments was freshly prepared using distilled water, in hydrochloric acid (obtained from the Scharlau Company, Analytical reagent grade 36%). The effect of temperature was studied on the corrosion process between (298.15-318.15) K by using a circulating water bath (HYSC company, Korea).

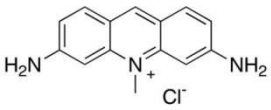


**Figure-1.**The chemical structure of acriflavine.

### 2.2. Electrochemical measurement

A suitable corrosion cell was designed in Pyrex glass that included five necks, with three necks accommodating the working electrode (carbon steel), a counter electrode and the reference electrode. The remaining necks allowed the entry and exit of nitrogen gas (purity 99.99%). The counter electrode was a platinum foil coated with black platinum to increase the surface area and catalytic activity [14].The reference electrode was a saturated Calomel electrode (Hg | $Hg_2Cl_{2(s)}$ | KCl) which was inserted in a Luggin capillary tube and the fine tip close to the electrode surface in corrosion cell to minimize the Ohmic potential drop [15]. After the assembly was complete all the poles were connected to a Potentiostat/Galvanostat Interface 1000 (supplied from GAMAY company, USA ) to measure the open circuit potential and to obtain the polarization curves. The Echem Analyst program was used to calculate the kinetic parameters for the Tafel polarization curves at a polarizing value ± 100 mV with respect to the free value of corrosion potential (*Evs.* SCE).

### 2.3. Surface Morphology

Scanning electron microscopy (SEM) was used to inspect the electrode surface in the absence and the presence of acriflavine inhibitor with silicon dioxide nanoparticles in 0.25 M HCl. The SEM was performed using a Type ZEISS sigma300 (Germany) with the following experimental parameters: resolution @ 1 kV (2.2 nm) , maximum scan speed (100 ns/pixel) and accelerating voltage (0.02 - 30 kV). Atomic force microscopy (AFM) was also performed (AA3000, Angstrom Advanced Inc. The USA) with the following parameters: 0.26 nm lateral resolution, 0.1 nm vertical resolution and precision of 50 nm. Measurements were made after immersion in 0.25M HCl acidic solution in the absence and the presence of$1 \times 10^{-3}$ M acriflavine + silica nanoparticles (0.05 g) at 298.15 K . Energy dispersive X-ray spectroscopy (Oxford Instruments, UK ) used to determine the chemical composition of protected layer. In all experiments, the specimens were washed in carefully with distilled water and then dried to examine without any further treatments.

## 3. RESULTS AND DISCUSSIONS

### 3.1. The open circuit potential (OCP)

It is important to stabilise the open circuit potential (OCP) before each experimental polarization scan. Thus, the measured values of OCP of the carbon steel working electrode as a function of time are used to define the areas of complete and partial inhibition of corrosion process as well determining the concentration of the inhibition threshold [16]. Figure-1 exhibits the fluctuation of the OCP of the carbon steel electrode with time in 0.25 M HCl acidic solution in the absence and the presence of various concentration of acriflavine inhibitor at 298.15 K. It is understood that the potential values of carbon steel electrode that was immersed in 0.25 M HCl without the addition of acriflavine inhibitor have a tendency to drift towards more negative potential values firstly, which led to a short step. This phenomenon was reported by West in previous articles[17], which represents the collapse (breakdown) of the oxide film formed in air before immersion displays on the surface according to equation (1) [18]:

$$Fe_2O_3 + 6HCl \rightarrow 2FeCl_3 + 3H_2O \quad (1)$$

It follows that to increase new oxide film in the solution so that the OCP values was changed slightly again to more noble direction to establish a possible condition of a steady state potential. On the other hand, in the presence of acriflavineinhibitor, the steady-state potential shifted towards the more positive value as shown in Figure-2. This behaviour can be explained in the idea of formation of a protective film within a certain thickness on the electrode surface of carbon steel [19,20].

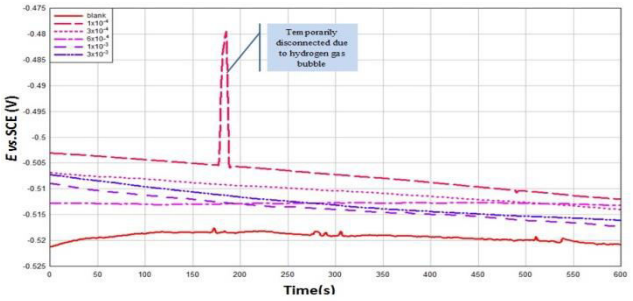


**Figure-2.** The potential circuit curves of carbon steel 0.5 M HCl at various concentrations of acriflavine inhibitor at 298.15 K.

### 3.2 Potentiodynamic polarization curves

Figure-3 shows the anodic and cathodic polarization scans of the carbon steel in 0.25 M HCl acidic solution in the absence and in the presence of different concentrations of acriflavine inhibitor at 298.15 K. It is clear that there is no significant change in the shape of the curve, but it can be seen that the current corrosion density values are displaced towards lower values as a result of increasing the inhibitor concentration. This is shown in

Table-2 which represents the electrochemical parameters that are obtained from Tafel lines.

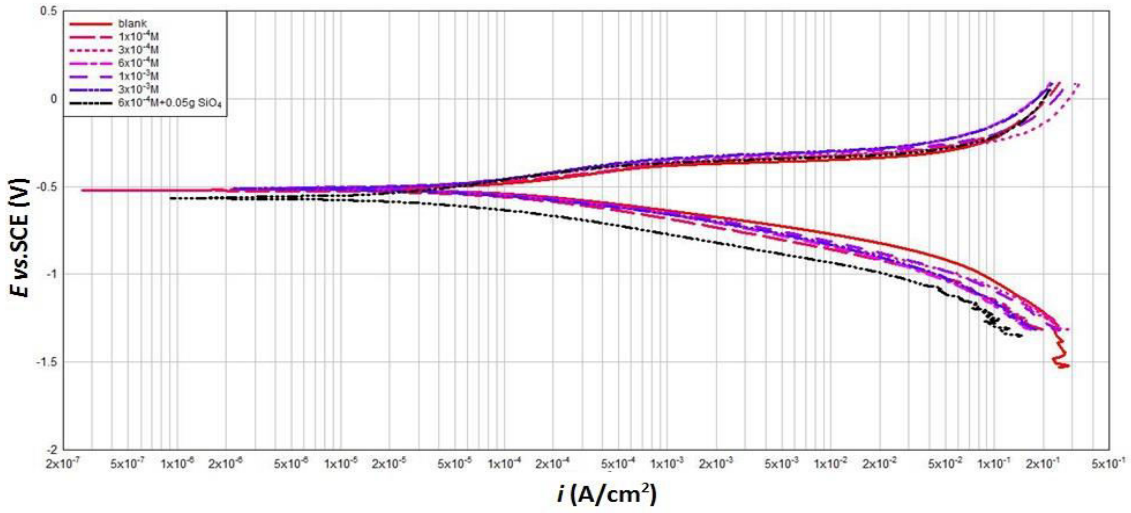


**Figure-3.**The potentiodynamic polarization curves of carbon steel in 0.5 M HCl with and without acriflavine inhibitor as well as in the presence of silica nanoparticles at 298.15 K.

**Table-2.** The kinetic parameters and inhibition efficiency of carbon steel in 0.5 M HCl at various concentrations of acriflavine inhibitor and in the presence of $SiO_2$ nanoparticle at 298.15 K.

| **Conc.** (M) | $i_{\text{Corr.}}$ ($\mu$A/cm$^2$) | $E_{\text{Corr.}}$ (mV) | $\beta_a$(mV/decade) | $\beta_c$ (mV/decade) | **Corrosion Rate** (mpy) | **%*IE*** | $\theta$ |
|---|---|---|---|---|---|---|---|
| blank | 100.0 | -516.0 | 155.0 | 121.0 | 37.12 | --- | --- |
| $1\times10^{-4}$ | 72.70 | -522.0 | 180.6 | 133.2 | 27.01 | 27.3 | 0.27 |
| $3\times10^{-4}$ | 57.50 | -511.0 | 145.2 | 104.0 | 21.35 | 42.3 | 0.42 |
| $6\times10^{-4}$ | 57.30 | -511.0 | 148.1 | 111.0 | 21.26 | 42.5 | 0.42 |
| $1\times10^{-3}$ | 52.10 | -510.0 | 150.3 | 100.1 | 19.36 | 47.9 | 0.47 |
| $3\times10^{-3}$ | 49.50 | -512.0 | 138.0 | 111.2 | 18.38 | 50.5 | 0.50 |
| 0.05 g $SiO_2$ nanoparticle | | | | | | | |
| $6\times10^{-4}$ | 15.30 | -566.0 | 125.0 | 81.30 | 5.678 | 84.70 | 0.84 |

The data from Table-2 illustrate the changes in corrosion potential towards the noble direction and the corrosion current density decrease is consistent with increasing the acriflavine concentration. The change in corrosion potential can be interpreted as being due to the adsorption of inhibitor molecules at the active sites of the surface of the carbon steel, causing a reduction in the rate of corrosion [21,22] as shown clearly in Table-2. Examination of these data also indicates that the addition of acriflavine inhibitor at various concentrations effects changes in the anodic and cathodic Tafel slopes. This behaviour reveals that acriflavine acts as mixed type inhibitor, in other words, the molecules of acriflavine inhibitor are adsorbed on both the cathodic and anodic sites and hence impede the cathodic reduction reaction and anodic dissolution[22], respectively.

The inhibition efficiencies and the degree of surface coverage are determined from equations (2) and (3), respectively[23,24] from the corrosion current density in the absence of inhibitor ($i_{\text{corr.uninh.}}$) and the presence of acriflavine inhibitor ($i_{\text{corr.inh.}}$) as shown in Table-2.

$$IE\% = \left(\frac{i_{\text{corr.uninh.}} - i_{\text{corr.inh.}}}{i_{\text{corr.uninh.}}}\right) \times 100 \quad (2)$$

$$\theta = \left(\frac{i_{\text{corr.uninh.}} - i_{\text{corr.inh.}}}{i_{\text{corr.uninh.}}}\right) \quad (3)$$

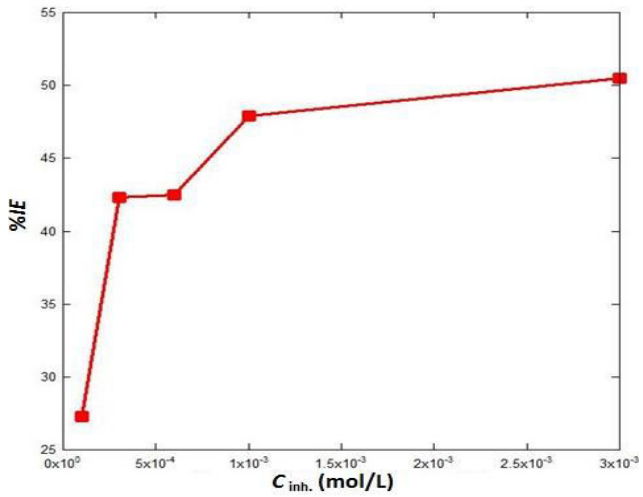


**Figure-4.** The relationship between the inhibition efficiency and concentration of acriflavine inhibitorin 0.5 M HCl solution at 298.15 K.

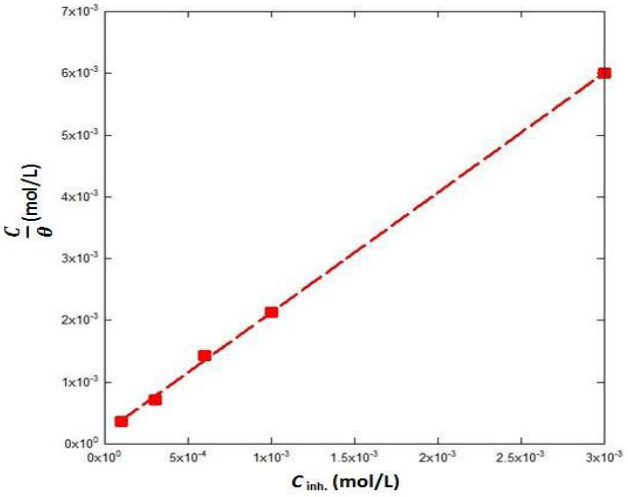


**Figure-5.** Langmuir adsorption plots of carbon steel in 0.5 M HCl solution at 298.15 K.

Form Table-2 and Figure-4 it is clear that the inhibition efficiencies increase with increasing acriflavine concentration, which is consistent with the values of the degree of surface coverage.

The Langmuir isotherm and standard free energy of adsorption ($\Delta G_{ads}$) equations that have been explained in previous articles[25,26] were used to infer the formation of a layer acriflavine molecules on the surface of the carbon steel electrode to confirm the adsorption process, which often occurs by displacement of water molecules [27]. The values of equilibrium constant $K_{ad}$ obtained from the Langmuir relationship and the $\Delta G_{ads}$ were 5319.14 $M^{-1}$ and -31.22kJ $mol^{-1}$, respectively with $r^2 = 1$ as shown in Figure-5. These results indicate the high adsorption of acriflavine inhibitor on the surface electrode and a good interaction between them which enhanced the phenomenon of mixed adsorption[28]. Thus, the negative value of adsorption obtained from the standard free energy equation refers to the spontaneity of adsorption process and the stability of the protecting layer [15,29].

The results that are shown in Table-2 and Figure-3 give a clear indication of the effect of silicon dioxide nanoparticles on the corrosion inhibition of carbon steel in 0.25 M HCl at 298.15 K, *i.e.* the reduction in the value of the corrosion current density of up to 15.3µA/$cm^2$ and the high value of the efficiency of corrosion inhibition to become 81.3%.In addition, large apparent changes can be observed in the value of anodic and cathodic Tafel slopes, Table-2. Consequently, all these data are consistent with the enhancement of corrosion inhibition by $SiO_2$ nanoparticles *via*strongly adsorbed molecules and the formation of a barrier film on the carbon steel surface. The result is a reduction in the rate anodic and cathodic processes, which is greater than it was the presence of the inhibitor alone, in the manner of Volmer- Tafel mechanism [30] and reduces the general corrosion rate.

### 3.3 The effect of temperature

The effect of temperature on the behaviour of the corrosion inhibition in absence and the presence of $3 \times 10^{-3}$ M of acriflavine inhibitor over temperature range (298.15-318.15) K was examined by acquiring potentiodynamic polarization scan as shown in Figure-6 A,B. The important kinetics parameters, which were obtained from Tafel lines, are listed in Table-3.

It is widely known when the temperature rises this results in an increase in the corrosion rate in the absence and the presence corrosion inhibitors. The data in Table-3 illustrate the corrosion current density for each temperature value decreases following the addition of acriflavine, but increases with increasing temperature. The corrosion efficiency increases with temperature up to 308.15 K. This observation may explained on the basis of the special interaction between inhibitor and the surface or by changing the nature of manner of adsorption[31],i.e. at lower temperatures this is a physical adsorption process, but when the temperature increases a chemical adsorption becomes more prevalent and more favourable. This phenomenon has been explained by other researchers[32],

as being due to the increased degree of coverage of the surface of the carbon steel electrode by inhibitor molecules. In other words, the rate determining step of carbon steel through dissolution in anodic reaction is controlled both by the diffusion inhibitor as well as corrosion products on the surface layer. At a temperature, with or without the acriflavine, the corrosion potential shifts to less negative values and this reflects the increase in corrosion resistance and enhanced inhibitory effect of acriflavine as shown in Table-3. Thus, the variation in the values of Tafel slopes at the same temperature in the absence and the presence of acriflavine (calculated from the polarization curve) suggests that the mechanism of corrosion inhibition is influenced by the addition of inhibitor and controlled by the cathodic and anodic reactions[33].

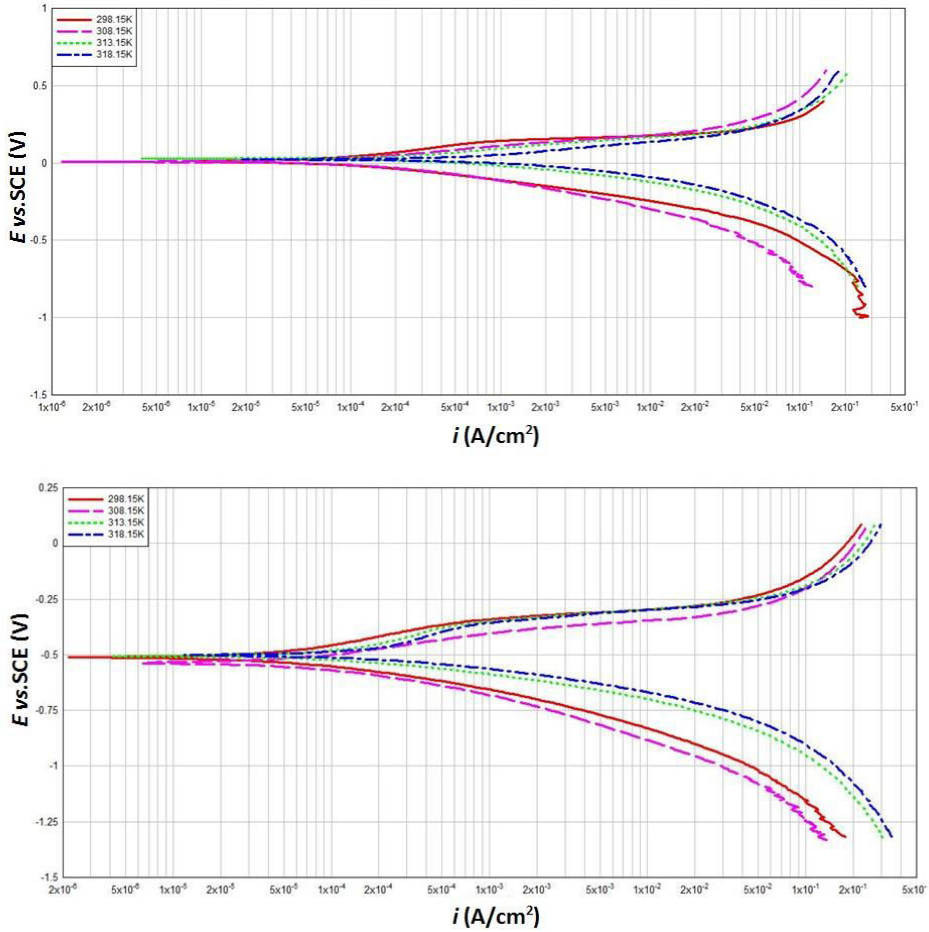


**Figure-6.** Potentiodynamic polarization curves of carbon steel in 0.5 M HCl in the absence (A) and in the presence of $3 \times 10^{-3}$ Macriflavine inhibitor in over range temperatures (298.15-318.15) K(B).

**Table-3.** The kinetic parameters and inhibition efficiency of carbon in 0.5 M HCl with $3 \times 10^{-3}$ Macriflavine inhibitor in over range temperatures(298.15-318.15) K.

| $T$(k) | $i_{Corr.}$ (μA/cm$^2$) | $E_{Corr.}$ (mV) | $\beta_a$ (mV/decade) | $\beta_c$ (mV/decade) | Corrosion Rate (mpy) | %$IE$ |
|---|---|---|---|---|---|---|
| Blank | | | | | | |
| 298.15 | 100.0 | -516.0 | 155.0 | 121.0 | 37.12 | --- |
| 308.15 | 104.0 | -569.0 | 109.8 | 115.3 | 38.42 | --- |
| 313.15 | 383.0 | -527.0 | 156.6 | 98.00 | 141.8 | --- |
| 318.15 | 844.0 | -514.0 | 126.0 | 101.3 | 312.3 | --- |
| **Acriflavine** | | | | | | |
| 298.15 | 49.50 | -512.0 | 138.0 | 111.2 | 18.38 | 50.50 |
| 308.15 | 70.70 | -536.0 | 138.0 | 118.1 | 26.14 | 32.01 |
| 313.15 | 135.0 | -505.0 | 122.7 | 93.20 | 49.90 | 64.75 |
| 318.15 | 266.0 | -502.0 | 226.8 | 96.00 | 98.32 | 68.48 |

In order to estimate the apparent activation energy [34]($E_a$) for corrosion process independently of the Arrhenius equation that described in below, equation (3a)

$$\log \text{corrosion rate} = \log A - \frac{-E_a}{2.303RT} \qquad (3a)$$

where $E_a$ is an apparent activation energy,$R$ is the universal gas constant, $T$ is the absolute temperature in Kelvin and $A$ represents the pre-exponential (collision) factor. The values of $E_a$ shown in Table-4 with and without acriflavine ($3 \times 10^{-3}$ M) over the temperature range (298.15-318.15) K were obtained by plotting the log corrosion rateversus ($1/T$) and are shown graphically in Figure-7.

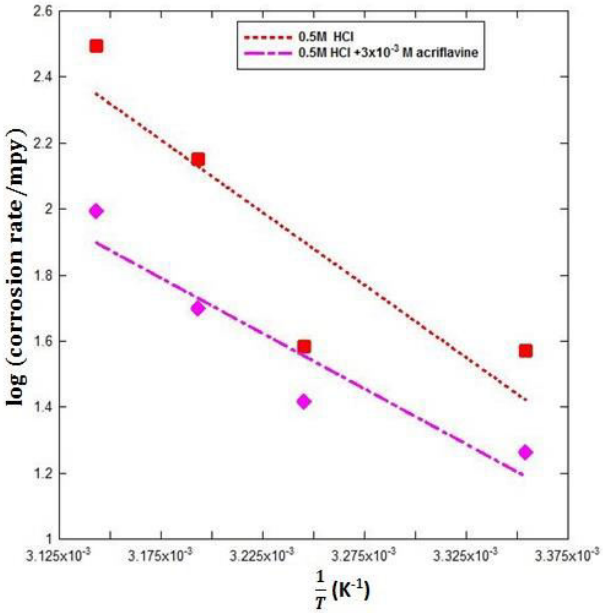


**Figure-7.**Arrhenius plots of carbon steel in the absence and the presence $3\times10^{-3}$ M of acriflavine in 0.5 M HCl solution.

**Table-4.** Thermodynamic and kinetic corrosion parameters in the absence and the presence$3\times10^{-3}$ M of acriflavine in 0.5 M HCl solution in over range temperatures(298.15-318.15) K.

| **Arrhenius equation** | | | | | |
|---|---|---|---|---|---|
| **Conc.**(M) | **r$^2$** | **Intercept** | **Slope** | $A$ **cm$^{-2}$s$^{-1}$** | $E_a$**kJ mol$^{-1}$** |
| blank | 0.767 | 16.16 | -4392 | 4527983.93 | 87.84 |
| $3 \times 10^{-3}$ | 0.949 | 14.18 | -3898 | 625175.300 | 77.96 |
| **Transition state equation** | | | | | |
| **Conc.**(M) | **r$^2$** | **Intercept** | **Slope** | $\Delta H_a$**kJ mol$^{-1}$** | $\Delta S_a$ **Jmol$^{-1}$K$^{-1}$** |
| blank | 0.756 | 13.24 | -4258 | 85.16 | 55.918 |
| $3 \times 10^{-3}$ | 0.880 | 9.517 | -3219 | 64.38 | -15.377 |

The transition - state equation [35] (4) was applied as a modified form of the Arrhenius equation to determine the enthalpy and entropy of activation.

$$\log\frac{\text{corrosion rate}}{T} = \log\frac{R}{Nh} + \left[\frac{\Delta S_a}{2.303R}\right] - \left[\frac{\Delta H_a}{2.303RT}\right] \quad (4)$$

$N$ represents Avogadro's number,$h$ is Planck's constant,$\Delta S_a$ is the entropy of activation and the $\Delta H_a$ is the enthalpy of activation. By plotting values of $\log\frac{\text{corrosion rate}}{T}$versus $(1/T)$ it is possible to estimate the $\Delta H_a$ and $\Delta S_a$ from the slope and intercept of above equation, respectively as shown in Table-4 and depicted graphically in Figure-8.

In the presence of acriflavine the value of apparent activation energy was reduced in comparison with the uninhibited solution, and this may be credited for the change of the mechanism for the corrosion reactions through the adsorption of the acriflavine molecules[36].Furthermore, the drop in the value of activation energy typically enhances the chemical adsorption that occurs [37]. Other researchers have pointed to the decrease in the activation energy value to show that the rate of adsorption of the inhibitor approaches equilibrium for the adsorption-desorption process at higher temperatures[36]. In addition to the reduction in the rates of the cathodic and anodic reactions on the surface electrode, parallel reactions can take place in the covered area, but in general, the rate of corrosion in the covered area is considerably lower than the uncovered area. Data from energy dispersive x-ray spectroscopy (EDS) and atomic force microscopy (AFM) corroborate the hypothesis that the inhibition of corrosion process on the surface carbon steel electrode occurs through the formation of a protective film.

The values of $r^2$ , which are close to unity (Table-4), refer to the corrosion process of carbon steel in 0.25 M HCl and may be interpreted on the basis of a kinetic model [38]. The positive value of enthalpy of activation indicates that the nature of carbon steel dissolution process is endothermic and decreases in the same manner with activation energy value and leads to a reduction in the corrosion rate that is typically related to the pre-exponential factor [39]. Thus, the large and negative values indicate at the rate determining step involves an activated complex as an association step rather than a dissociation step, because of the increase in entropy [40]. The findings agree with literature findings[41,42].

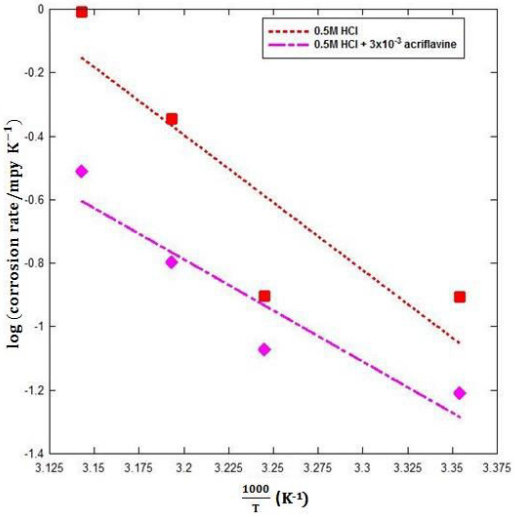


**Figure-8.**Plot of variation $\log\frac{\text{corrosion rate}}{T}$ vs. 1000/$T$.

### 3.4 Study the morphology surface of carbon steel

The corrosion behaviour of carbon steel in 0.5 M HCl in the absence and the presence of $6\times10^{-4}$M acriflavine with 0.05g silica nanoparticle at 298.15 K was inspected by scanning electron microscopy (SEM), Energy - dispersive X-ray spectroscopy (EDS) and atomic force microscope (AFM) without any further treatment.

#### 3.4.1 SEM and EDX characterization

Figure-9-a shows the morphology surface of carbon steel in 0.5 M HCl in the absence of $6\times10^{-4}$ M acriflavine with the 0.05g silicon dioxide nanoparticle, indicating the characteristic uniform roughness of the surface and the formation of the corrosion products (cracks and pits) on the electrode's surface. The corrosion product (corrosion film) which is evident as the colour whitened from black to grey, is characteristic of a $Fe_3C$ film [43]. Moreover, the EDX analysis revealed the surface composition to be elemental iron (79.5%) and carbon (20.5%). In the presence of the silicon dioxide and acriflavine (Figure-9-b), there appears to be less roughness and the pitting has disappeared, in addition to at least the appearance of sharp cracks, indicating the formation of protected film adsorbed on the electrode's surface. The adsorbed material acts as a passivating layer to block the active sites and reduce the corrosion rate by decreasing the contact between the surface electrode and the aggressive acidic solution. Furthermore, the chemical analysis of composition surface electrode indicates that the percentage of elemental iron has decreased to 74.8% and the carbon content is now 15.5%. The appearance of some elements, such as manganese, indicates that the protection layer contains alloys of these elements with oxygen.

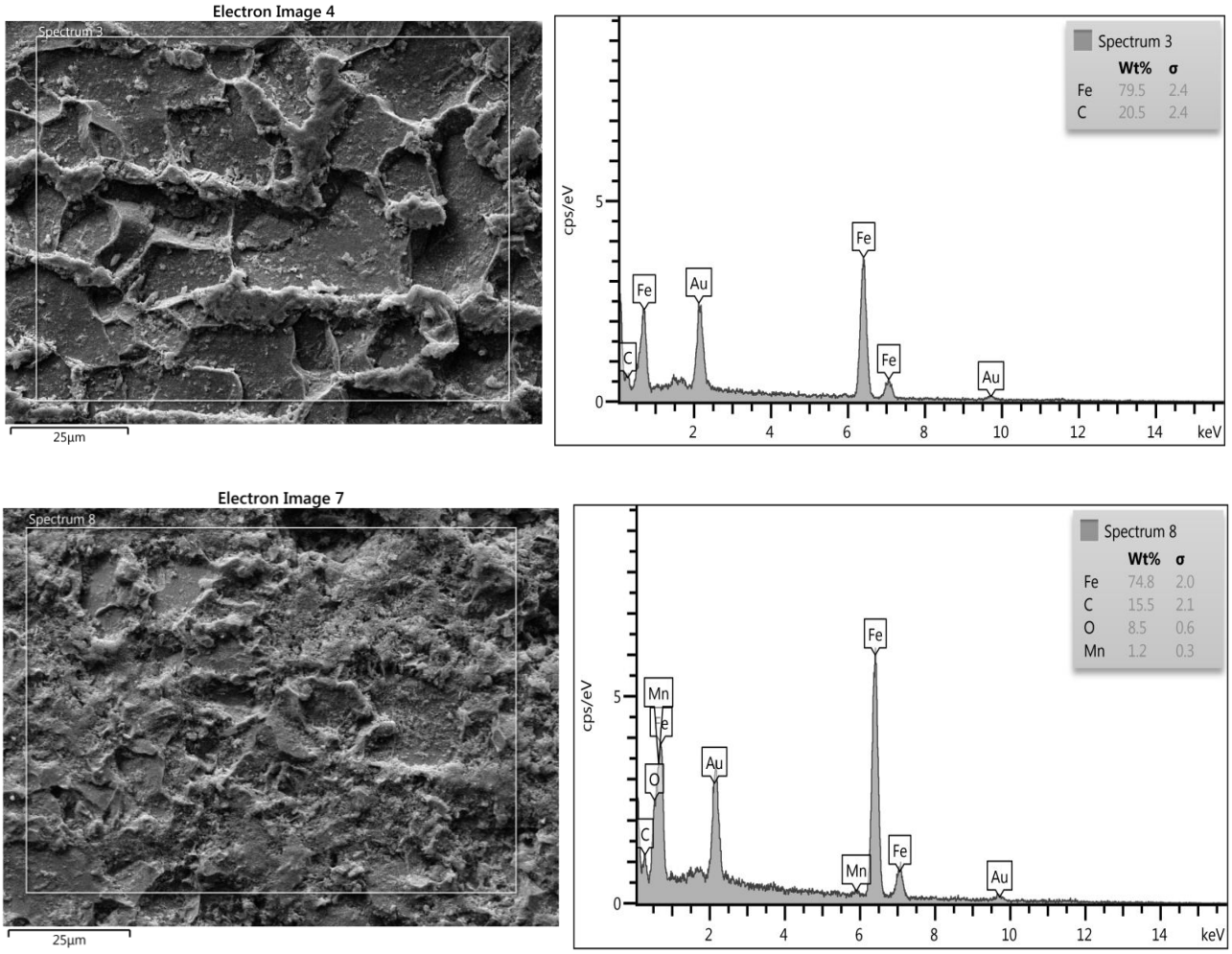


**Figure-9.**The SEM and EDS for the carbon steel electrode surface in (a) 0.5 M HCl (blank solution) and (b) The presence of silica nanoparticles with acriflavine inhibitor at 298.15 K.

### 3.4.2 AFM characterization

The atomic force microscope is an important tool to characterize the surface of the electrodes and the two- and three-dimensional AFM images were depicted in Figure (10 a, b and c). It is possible to note from Figure-10-a that the polished surface of the carbon steel electrode is somewhat soft and displays a regular topography. The average roughness value ($R_a$) is around 23 nm and after the electrode has been immersed in 0.25 M HCl for 48h in the absence of acriflavine, but with silicate nanoparticles as shown in Figure-10-b, cracks appear in addition to the irregular topography ($R_a$ rises to 71 nm) and this is attributed to the attack of the acid on the carbon steel. In the presence of the silica nanoparticles and acriflavine (Figure-10-c, the average roughness value is now 57 nm with a smoother surface. This inhibition effect is believed to be a result of the reduction in corrosion damage by the formation of a protective layer on the carbon steel surface and decreasing the contact between the steel and the aggressive acidic solution.

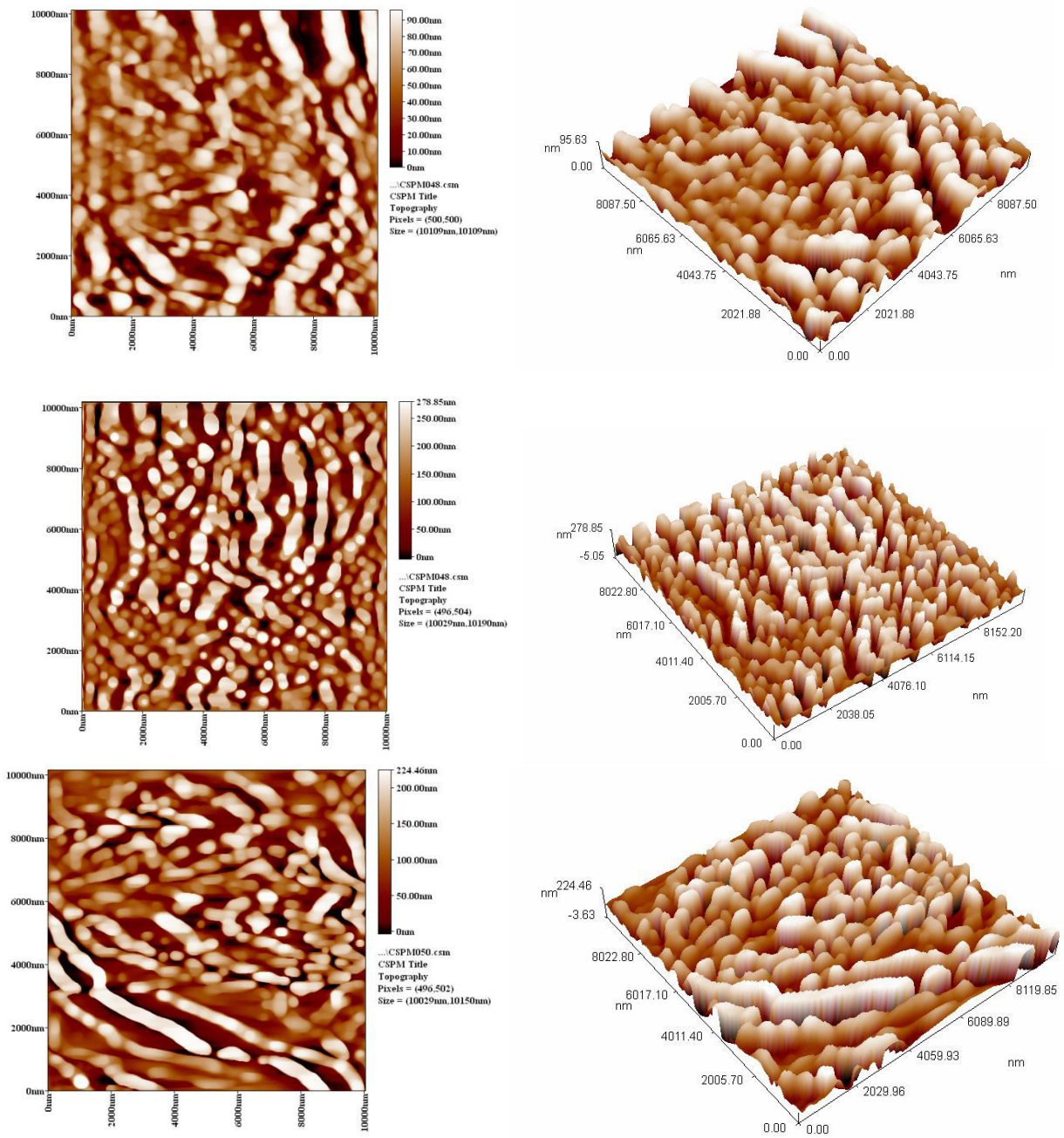


**Figure-10.** The AFM images in 2D and 3D of polish the carbon steel surface (a),0.5 M HCl (b) and the in presence silica nanoparticles with acriflavine inhibitor(c).

### 3.5 Mechanism of inhibition

Clarification of the inhibition mechanism requires full knowledge of the interaction of the compound inhibitor and the metal surface. Acriflavine performed as a mixed type inhibitor that blocked the active sites on the surface of carbon steel by becoming adsorbed on it to form a protective layer. Thus, the metal, which contained the active surface, was covered and both the cathodic and anodic current densities and then corrosion rate could be reduced. Firstly, in order to explain the mechanism of inhibition it is essential to mentionall the half-reactions, the anodic dissociation of iron for carbon steel and the cathodic reaction which includes evolution of hydrogen gas in the acidic medium. Thus, the equations for both the anodic (6 -9) and the cathodic reactions (10 - 12), which were proposed by Morad *et al.*[44] are described below.

$$Fe + Cl^- \rightleftarrows [FeCl^-]_{ads.} \quad (5)$$

$$[FeCl^-]_{ads.} \rightleftarrows [FeCl]_{ads.} + e^- \quad (6)$$

$$[FeCl]_{ads.} \rightleftarrows [FeCl^+]_{ads.} + e^- \quad (7)$$

$$[FeCl^+]_{ads.} \rightleftarrows Fe^{2+} + Cl^- \quad (8)$$

$$Fe + H^+ \rightleftarrows [FeH^+]_{ads.} \quad (9)$$

$$[FeH^+]_{ads.} + e^- \rightleftarrows [FeH]_{ads.} \quad (10)$$

$$[FeH]_{ads.} + H^+ + e^- \rightleftarrows Fe + H_2 \uparrow \quad (11)$$

Generally, when the concentration of acriflavine was increased then the inhibition efficiency at constant temperature decreased, as a result, to inhibit the action of the corrosion process due to adsorption on the carbon steel surface. Thus, the structure of acriflavine shown in Figure-1 as a protonated molecule *via* nitrogen atom in the heterocyclic ring facilitates an electrostatic interaction [45] between acriflavine and the $[FeCl^-]_{ads.}$species as well as the formation of a dative covalent bond between electron pairs on the nitrogen atoms and vacant orbitals on the metal surface. Furthermore, acriflavine molecules are chemically adsorbed through the overlapping between the $\pi$-orbitals with the d-orbital in iron atom. In the present research, the value of the standard free energy of adsorption is equal to -32.22 kJ $mol^{-1}$, indicating that the adsorption of acriflavine molecules on the surface electrode comprises both physisorption and chemisorption processes. This behaviour is favoured and remains consistent at constant temperature[46].

## 4. CONCLUSIONS

The following points are the most important conclusions:

a) Acriflavine acts as a good inhibitor for the corrosion reaction of carbon steel in 0.25 M HCl solution.
b) The open circuit potential values drifted slightly towards the positive direction in addition of acriflavine inhibitor, an indication of the increase in corrosion resistance. The results of potentiodynamic polarization measurements confirm that the corrosion rate is reduced due to both the cathodic and anodic reactions becoming retarded as well as the acriflavine performing as a mixed-type inhibitor.
c) The inhibition efficiency of acriflavine increased over the temperature range (298.15-318.15) K, which leads to a decrease of the activation energy value for the corrosion process.
d) The acriflavine adsorption on the surface electrode obeys the Langmuir isotherm with a high value of $K_{ads}$, indicating a strong adsorption on the surface of the electrode.
e) The positive value for the $\Delta H_a$ refers to an endothermic process, and the negative value of entropy confirms that the formation of an activated complex is involved.
f) The effect of silicon nanoparticles is explained and the corrosion inhibition exceeds 80%, which confirms an improvement in the protective adsorption layer thus reducing the rate of corrosion. These results are further reinforced by characterization of the surface morphology of the electrode

## REFERENCES

[1] Jawich MWS, Oweimreen GA, Ali SA. 2012. Heptadecyl-tailed mono- and bis-imidazolines: A study of the newly synthesized compounds on the inhibition of mild steel corrosion in a carbon dioxide-saturated saline medium. Corros Sci. 65:104-112.

[2] Li L, Zhang X, Lei J, et al (2012) Adsorption and corrosion inhibition of Osmanthus fragran leaves extract on carbon steel. Corros Sci. 63:82-90.

[3] Alaoui Mouayd A, Orazem ME, Sutter EMM, et al. 2014. Contribution of electrochemical dissolution during pickling of low carbon steel in acidic solutions. Corros Sci. 82:362-368.

[4] Ayyannan G, Karthikeyan K, Vivekananthan SS, et al. 2013. Chemical and electrochemical investigations of high carbon steel corrosion inhibition in 10 % HCl medium by quinoline chalcones. Ionics (Kiel). 19:919-932.

[5] Nešić S. 2007. Key issues related to modelling of internal corrosion of oil and gas pipelines - A review. Corros Sci. 49:4308-4338.

[6] Del Angel-Lpez D, Domnguez-Crespo MA, Torres-Huerta AM, *et al.* 2013. Analysis of degradation process during the incorporation of ZrO 2:SiO2 ceramic nanostructures into polyurethane coatings for the corrosion protection of carbon steel. J Mater Sci. 48:1067-1084.

[7] Ramalingam S, Muralidharan VS, Subramania A. 2009. Electrodeposition and characterization of Cu-TiO2 nanocomposite coatings. J Solid State Electrochem. 13:1777-1783.

[8] Clapsaddle BJ, Gash AE, Satcher JH, Simpson RL. 2003. Silicon oxide in an iron (III) oxide matrix: The sol-gel synthesis and characterization of Fe-Si mixed oxide nanocomposites that contain iron oxide as the major phase. J Non Cryst Solids. 331:190-201.

[9] Amirdehi MF, Afzali D. 2013. Deposition of Polyaniline/Silica Nanocomposite Coating on Stainless Steel; Study of its Corrosion Properties. Adv Mater Res. 829:605-609.

[10] Trabelsi W, Cecilio P, Ferreira MGS, Montemor MF. 2005. Electrochemical assessment of the self-healing properties of Ce-doped silane solutions for the pre-

treatment of galvanised steel substrates. Prog Org Coatings. 54:276-284.

[11] Song Y, Yu J, Dai D, *et al.* 2014. Effect of silica particles modified by in-situ and ex-situ methods on the reinforcement of silicone rubber. Mater Des. 64:687-693.

[12] Joo SH, Park JY, Tsung C-K, *et al.* 2009. Thermally stable Pt/mesoporous silica core-shell nanocatalysts for high-temperature reactions. Nat Mater. 8:126-31.

[13] Hedayati M, Salehi M, Bagheri R, *et al.* 2011. Tribological and mechanical properties of amorphous and semi-crystalline PEEK/SiO2 nanocomposite coatings deposited on the plain carbon steel by electrostatic powder spray technique. Prog Org Coatings. 74:50-58.

[14] Ghasemi Z, Tizpar A. 2006. The inhibition effect of some amino acids towards Pb-Sb-Se-As alloy corrosion in sulfuric acid solution. Appl Surf Sci. 252:3667-3672.

[15] Ochoa N, Moran F, Pébère N, Tribollet B. 2005. Influence of flow on the corrosion inhibition of carbon steel by fatty amines in association with phosphonocarboxylic acid salts. Corros Sci. 47:593-604.

[16] Zhao Z, Castanheira L, Dubau L, *et al.* 2013. Carbon corrosion and platinum nanoparticles ripening under open circuit potential conditions. J Power Sources. 230:236-243.

[17] Migahed MA, Nassar IF. 2008. Corrosion inhibition of Tubing steel during acidization of oil and gas wells. Electrochim Acta. 53:2877-2882.

[18] Gilroy D, Mayne JEO. 1965. The breakdown of the air-formed oxide film on iron upon immersion in solutions of pH 6-13. Br Corros J. 1:102-106.

[19] Romaine A, Jeannin M, Sabot R, *et al.* 2015. Corrosion processes of carbon steel in argillite: Galvanic effects associated with the heterogeneity of the corrosion product layer. Electrochim Acta. 182:1019-1028.

[20] Wang G, Zhang L, Zhang J. 2012. A review of electrode materials for electrochemical supercapacitors. Chem Soc Rev. 41:797.

[21] Thanapackiam P, Rameshkumar S, Subramanian SS, Mallaiya K. 2016. Electrochemical evaluation of inhibition efficiency of ciprofloxacin on the corrosion of copper in acid media. Mater Chem Phys. 174:129-137.

[22] El-Deeb MM, Sayyah SM, Abd El-Rehim SS, Mohamed SM. 2013. Corrosion inhibition of aluminum with a series of aniline monomeric surfactants and their analog polymers in 0.5 M HCl solution. Part II: 3-(12-sodiumsulfonate dodecyloxy) aniline and its analog polymer. Arab J Chem. 8:527-537.

[23] Deyab MA, Dief HAA, Eissa EA, Taman AR. 2007. Electrochemical investigations of naphthenic acid corrosion for carbon steel and the inhibitive effect by some ethoxylated fatty acids. Electrochim Acta. 52:8105-8110.

[24] Şahin M, Bilgiç S, Yilmaz H. 2002. The inhibition effects of some cyclic nitrogen compounds on the corrosion of the steel in NaCl mediums. Appl Surf Sci. 195:1-7.

[25] Langmuir I. 1916.The Constitution and Fundamental Properties of Solids and Liquids. Part I. Solids. J Am Chem Soc. 38:2221-2295.

[26] Zhang QB, Hua YX. 2009. Corrosion inhibition of mild steel by alkylimidazolium ionic liquids in hydrochloric acid. Electrochim Acta. 54:1881-188727.

[27] Singh AK, Quraishi MA. 2010. Effect of Cefazolin on the corrosion of mild steel in HCl solution. Corros Sci. 52:152-160.

[28] Solmaz R, Karda\cs G, Culha M, *et al.* 2008. Investigation of adsorption and inhibitive effect of 2-mercaptothiazoline on corrosion of mild steel in hydrochloric acid media. Electrochim Acta. 53:5941-5952.

[29] El-Etre AY. 2006. Khillah extract as inhibitor for acid corrosion of SX 316 steel. Appl Surf Sci. 252:8521-8525.

[30] Kellenberger A, Vaszilcsin N, Brandl W, Duteanu N. 2007. Kinetics of hydrogen evolution reaction on skeleton nickel and nickel-titanium electrodes obtained by thermal arc spraying technique. Int J Hydrogen Energy. 32:3258-3265.

[31] Bouklah M, Hammouti B, Lagren??e M, Bentiss F. 2006. Thermodynamic properties of 2,5-bis(4-

methoxyphenyl)-1,3,4-oxadiazole as a corrosion inhibitor for mild steel in normal sulfuric acid medium. Corros Sci. 48:2831-2842.

[32] Oguzie EE, Li Y, Wang FH. 2007. Corrosion inhibition and adsorption behavior of methionine on mild steel in sulfuric acid and synergistic effect of iodide ion. J Colloid Interface Sci. 310:90-98.

[33] Solmaz R. 2014. Investigation of adsorption and corrosion inhibition of mild steel in hydrochloric acid solution by 5- (4-Dimethylaminobenzylidene) rhodanine. Corros Sci. 79:169-176.

[34] Khadraoui A, Khelifa A, Hamitouche H, Mehdaoui R. 2014. Inhibitive effect by extract of Mentha rotundifolia leaves on the corrosion of steel in 1 M HCl solution. Res Chem Intermed. 40:961-972.

[35] Deyab MA, El-Rehim SSA. 2014. Effect of succinic acid on carbon steel corrosion in produced water of crude oil. J Taiwan Inst Chem Eng. 45:1065-1072.

[36] Singh AK, Quraishi MA. 2011. Adsorption properties and inhibition of mild steel corrosion in hydrochloric acid solution by ceftobiprole. J Appl. Electrochem. 41:7-18.

[37] Tang Y, Zhang F, Hu S, *et al.* 2013. Novel benzimidazole derivatives as corrosion inhibitors of mild steel in the acidic media. Part I: Gravimetric, electrochemical, SEM and XPS studies. Corros Sci. 74:271-282.

[38] Fiori-Bimbi M V., Alvarez PE, Vaca H, Gervasi CA. 2015. Corrosion inhibition of mild steel in HCL solution by pectin. Corros Sci. 92:192-199.

[39] Abd-Elaal AA, Aiad I, Shaban SM, *et al.* 2014. Synthesis and evaluation of some Triazole derivatives as corrosion inhibitors and biocides. J Surfactants Deterg. 17:483-491.

[40] Singh AK, Quraishi MA. 2010. Inhibitive effect of diethylcarbamazine on the corrosion of mild steel in hydrochloric acid. Corros Sci. 52:1529-1535.

[41] Tang L, Mu G, Liu G. 2003. The effect of neutral red on the corrosion inhibition of cold rolled steel in 1.0 M hydrochloric acid. Corros Sci. 45:2251-2262.

[42] Zhang QB, Hua YX. 2009. Corrosion inhibition of mild steel by alkylimidazolium ionic liquids in hydrochloric acid. Electrochim Acta. 54:1881-1887.

[43] Li XJ, He LL, Li YS, *et al.* 2014. TEM interfacial characterization of CVD diamond film grown on Al inter-layered steel substrate. Diam Relat Mater. 50:103-109.

[44] Morad MS, El-Dean AMK. 2006. 2,2-Dithiobis(3-cyano-4,6-dimethylpyridine): A new class of acid corrosion inhibitors for mild steel. Corros Sci. 48:3398-3412.

[45] Ongun Yce A, Doru Mert B, Karda G, Yazici B. 2014. Electrochemical and quantum chemical studies of 2-amino-4-methyl-thiazole as corrosion inhibitor for mild steel in HCl solution. Corros Sci. 83:310-316.

[46] Issaadi S, Douadi T, Zouaoui A, *et al.* 2011. Novel thiophene symmetrical Schiff base compounds as corrosion inhibitor for mild steel in acidic media. Corros Sci. 53:1484-1488.